



CERN-PH-EP-2013-156

LHCb-PAPER-2013-052

30 August, 2013

Study of J/ψ production and cold nuclear matter effects in $p\text{Pb}$ collisions

The LHCb collaboration[†]

Abstract

The production of J/ψ mesons with rapidity $1.5 < y < 4.0$ or $-5.0 < y < -2.5$ and transverse momentum $p_T < 14 \text{ GeV}/c$ is studied with the LHCb detector in proton-lead collisions at a proton-nucleon centre-of-mass energy $\sqrt{s_{NN}} = 5 \text{ TeV}$. The analysis is based on a data sample corresponding to an integrated luminosity of about 1.6 nb^{-1} . For the first time the nuclear modification factor and forward-backward production ratio are determined separately for J/ψ mesons originating directly from the proton-nucleon collision and from b -hadron decays.

Submitted to JHEP

© CERN on behalf of the LHCb collaboration, license CC-BY-3.0.

[†]Authors are listed on the following pages.

LHCb collaboration

R. Aaij⁴⁰, B. Adeva³⁶, M. Adinolfi⁴⁵, C. Adrover⁶, A. Affolder⁵¹, Z. Ajaltouni⁵, J. Albrecht⁹, F. Alessio³⁷, M. Alexander⁵⁰, S. Ali⁴⁰, G. Alkhazov²⁹, P. Alvarez Cartelle³⁶, A.A. Alves Jr^{24,37}, S. Amato², S. Amerio²¹, Y. Amhis⁷, L. Anderlini^{17,f}, J. Anderson³⁹, R. Andreassen⁵⁶, J.E. Andrews⁵⁷, R.B. Appleby⁵³, O. Aquines Gutierrez¹⁰, F. Archilli¹⁸, A. Artamonov³⁴, M. Artuso⁵⁸, E. Aslanides⁶, G. Auriemma^{24,m}, M. Baalouch⁵, S. Bachmann¹¹, J.J. Back⁴⁷, A. Badalov³⁵, C. Baesso⁵⁹, V. Balagura³⁰, W. Baldini¹⁶, R.J. Barlow⁵³, C. Barschel³⁷, S. Barsuk⁷, W. Barter⁴⁶, Th. Bauer⁴⁰, A. Bay³⁸, J. Beddow⁵⁰, F. Bedeschi²², I. Bediaga¹, S. Belogurov³⁰, K. Belous³⁴, I. Belyaev³⁰, E. Ben-Haim⁸, G. Bencivenni¹⁸, S. Benson⁴⁹, J. Benton⁴⁵, A. Berezhnoy³¹, R. Bernet³⁹, M.-O. Bettler⁴⁶, M. van Beuzekom⁴⁰, A. Bien¹¹, S. Bifani⁴⁴, T. Bird⁵³, A. Bizzeti^{17,h}, P.M. Bjørnstad⁵³, T. Blake³⁷, F. Blanc³⁸, J. Blouw¹⁰, S. Blusk⁵⁸, V. Bocci²⁴, A. Bondar³³, N. Bondar²⁹, W. Bonivento¹⁵, S. Borghi⁵³, A. Borgia⁵⁸, T.J.V. Bowcock⁵¹, E. Bowen³⁹, C. Bozzi¹⁶, T. Brambach⁹, J. van den Brand⁴¹, J. Bressieux³⁸, D. Brett⁵³, M. Britsch¹⁰, T. Britton⁵⁸, N.H. Brook⁴⁵, H. Brown⁵¹, A. Bursche³⁹, G. Busetto^{21,q}, J. Buytaert³⁷, S. Cadeddu¹⁵, O. Callot⁷, M. Calvi^{20,j}, M. Calvo Gomez^{35,n}, A. Camboni³⁵, P. Campana^{18,37}, D. Campora Perez³⁷, A. Carbone^{14,c}, G. Carboni^{23,k}, R. Cardinale^{19,i}, A. Cardini¹⁵, H. Carranza-Mejia⁴⁹, L. Carson⁵², K. Carvalho Akiba², G. Casse⁵¹, L. Cassina¹, L. Castillo Garcia³⁷, M. Cattaneo³⁷, Ch. Cauet⁹, R. Cenci⁵⁷, M. Charles⁵⁴, Ph. Charpentier³⁷, S.-F. Cheung⁵⁴, N. Chiapolini³⁹, M. Chrzasczcz^{39,25}, K. Ciba²⁶, X. Cid Vidal³⁷, G. Ciezarek⁵², P.E.L. Clarke⁴⁹, M. Clemencic³⁷, H.V. Cliff⁴⁶, J. Closier³⁷, C. Coca²⁸, V. Coco⁴⁰, J. Cogan⁶, E. Cogneras⁵, P. Collins³⁷, A. Comerma-Montells³⁵, A. Contu^{15,37}, A. Cook⁴⁵, M. Coombes⁴⁵, S. Coquereau⁸, G. Corti³⁷, B. Couturier³⁷, G.A. Cowan⁴⁹, D.C. Craik⁴⁷, S. Cunliffe⁵², R. Currie⁴⁹, C. D'Ambrosio³⁷, P. David⁸, P.N.Y. David⁴⁰, A. Davis⁵⁶, I. De Bonis⁴, K. De Bruyn⁴⁰, S. De Capua⁵³, M. De Cian¹¹, J.M. De Miranda¹, L. De Paula², W. De Silva⁵⁶, P. De Simone¹⁸, D. Decamp⁴, M. Deckenhoff⁹, L. Del Buono⁸, N. Deléage⁴, D. Derkach⁵⁴, O. Deschamps⁵, F. Dettori⁴¹, A. Di Canto¹¹, H. Dijkstra³⁷, M. Dogaru²⁸, S. Donleavy⁵¹, F. Dordei¹¹, A. Dosil Suárez³⁶, D. Dossett⁴⁷, A. Dovbnya⁴², F. Dupertuis³⁸, P. Durante³⁷, R. Dzhelyadin³⁴, A. Dziurda²⁵, A. Dzyuba²⁹, S. Easo⁴⁸, U. Egede⁵², V. Egorychev³⁰, S. Eidelman³³, D. van Eijk⁴⁰, S. Eisenhardt⁴⁹, U. Eitschberger⁹, R. Ekelhof⁹, L. Eklund^{50,37}, I. El Rifai⁵, Ch. Elsasser³⁹, A. Falabella^{14,e}, C. Färber¹¹, C. Farinelli⁴⁰, S. Farry⁵¹, D. Ferguson⁴⁹, V. Fernandez Albor³⁶, F. Ferreira Rodrigues¹, M. Ferro-Luzzi³⁷, S. Filippov³², M. Fiore^{16,e}, C. Fitzpatrick³⁷, M. Fontana¹⁰, F. Fontanelli^{19,i}, R. Forty³⁷, O. Francisco², M. Frank³⁷, C. Frei³⁷, M. Frosini^{17,37,f}, E. Furfaro^{23,k}, A. Gallas Torreira³⁶, D. Galli^{14,c}, M. Gandelman², P. Gandini⁵⁸, Y. Gao³, J. Garofoli⁵⁸, P. Garosi⁵³, J. Garra Tico⁴⁶, L. Garrido³⁵, C. Gaspar³⁷, R. Gauld⁵⁴, E. Gersabeck¹¹, M. Gersabeck⁵³, T. Gershon⁴⁷, Ph. Ghez⁴, V. Gibson⁴⁶, L. Giubega²⁸, V.V. Gligorov³⁷, C. Göbel⁵⁹, D. Golubkov³⁰, A. Golutvin^{52,30,37}, A. Gomes², P. Gorbounov^{30,37}, H. Gordon³⁷, M. Grabalosa Gándara⁵, R. Graciani Diaz³⁵, L.A. Granado Cardoso³⁷, E. Graugés³⁵, G. Graziani¹⁷, A. Grecu²⁸, E. Greening⁵⁴, S. Gregson⁴⁶, P. Griffith⁴⁴, O. Grünberg⁶⁰, B. Gui⁵⁸, E. Gushchin³², Yu. Guz^{34,37}, T. Gys³⁷, C. Hadjivasiliou⁵⁸, G. Haefeli³⁸, C. Haen³⁷, S.C. Haines⁴⁶, S. Hall⁵², B. Hamilton⁵⁷, T. Hampson⁴⁵, S. Hansmann-Menzemer¹¹, N. Harnew⁵⁴, S.T. Harnew⁴⁵, J. Harrison⁵³, T. Hartmann⁶⁰, J. He³⁷, T. Head³⁷, V. Heijne⁴⁰, K. Hennessy⁵¹, P. Henrard⁵, J.A. Hernando Morata³⁶, E. van Herwijnen³⁷, M. Heß⁶⁰, A. Hicheur¹, E. Hicks⁵¹, D. Hill⁵⁴, M. Hoballah⁵, C. Hombach⁵³, W. Hulsbergen⁴⁰, P. Hunt⁵⁴, T. Huse⁵¹, N. Hussain⁵⁴, D. Hutchcroft⁵¹, D. Hynds⁵⁰, V. Iakovenko⁴³, M. Idzik²⁶, P. Ilten¹², R. Jacobsson³⁷, A. Jaeger¹¹,

E. Jans⁴⁰, P. Jaton³⁸, A. Jawahery⁵⁷, F. Jing³, M. John⁵⁴, D. Johnson⁵⁴, C.R. Jones⁴⁶,
 C. Joram³⁷, B. Jost³⁷, M. Kaballo⁹, S. Kandybei⁴², W. Kanso⁶, M. Karacson³⁷, T.M. Karbach³⁷,
 I.R. Kenyon⁴⁴, T. Ketel⁴¹, B. Khanji²⁰, O. Kochebina⁷, I. Komarov³⁸, R.F. Koopman⁴¹,
 P. Koppenburg⁴⁰, M. Korolev³¹, A. Kozlinskiy⁴⁰, L. Kravchuk³², K. Kreplin¹¹, M. Kreps⁴⁷,
 G. Krocker¹¹, P. Krokovny³³, F. Kruse⁹, M. Kucharczyk^{20,25,37,j}, V. Kudryavtsev³³, K. Kurek²⁷,
 T. Kvaratskheliya^{30,37}, V.N. La Thi³⁸, D. Lacarrere³⁷, G. Lafferty⁵³, A. Lai¹⁵, D. Lambert⁴⁹,
 R.W. Lambert⁴¹, E. Lanciotti³⁷, G. Lanfranchi¹⁸, C. Langenbruch³⁷, T. Latham⁴⁷,
 C. Lazzeroni⁴⁴, R. Le Gac⁶, J. van Leerdam⁴⁰, J.-P. Lees⁴, R. Lefèvre⁵, A. Leflat³¹,
 J. Lefrançois⁷, S. Leo²², O. Leroy⁶, T. Lesiak²⁵, B. Leverington¹¹, Y. Li³, L. Li Gioi⁵, M. Liles⁵¹,
 R. Lindner³⁷, C. Linn¹¹, B. Liu³, G. Liu³⁷, S. Lohn³⁷, I. Longstaff⁵⁰, J.H. Lopes²,
 N. Lopez-March³⁸, H. Lu³, D. Lucchesi^{21,q}, J. Luisier³⁸, H. Luo⁴⁹, O. Lupton⁵⁴, F. Machefert⁷,
 I.V. Machikhiliyan³⁰, F. Maciuc²⁸, O. Maev^{29,37}, S. Malde⁵⁴, G. Manca^{15,d}, G. Mancinelli⁶,
 J. Maratas⁵, U. Marconi¹⁴, P. Marino^{22,s}, R. Märki³⁸, J. Marks¹¹, G. Martellotti²⁴, A. Martens⁸,
 A. Martín Sánchez⁷, M. Martinelli⁴⁰, D. Martinez Santos^{41,37}, D. Martins Tostes²,
 A. Martynov³¹, A. Massafferri¹, R. Matev³⁷, Z. Mathe³⁷, C. Matteuzzi²⁰, E. Maurice⁶,
 A. Mazurov^{16,32,37,e}, J. McCarthy⁴⁴, A. McNab⁵³, R. McNulty¹², B. McSkelly⁵¹,
 B. Meadows^{56,54}, F. Meier⁹, M. Meissner¹¹, M. Merk⁴⁰, D.A. Milanes⁸, M.-N. Minard⁴,
 J. Molina Rodriguez⁵⁹, S. Monteil⁵, D. Moran⁵³, P. Morawski²⁵, A. Mordà⁶, M.J. Morello^{22,s},
 R. Mountain⁵⁸, I. Mous⁴⁰, F. Muheim⁴⁹, K. Müller³⁹, R. Muresan²⁸, B. Muryn²⁶, B. Muster³⁸,
 P. Naik⁴⁵, T. Nakada³⁸, R. Nandakumar⁴⁸, I. Nasteva¹, M. Needham⁴⁹, S. Neubert³⁷,
 N. Neufeld³⁷, A.D. Nguyen³⁸, T.D. Nguyen³⁸, C. Nguyen-Mau^{38,o}, M. Nicol⁷, V. Niess⁵,
 R. Niet⁹, N. Nikitin³¹, T. Nikodem¹¹, A. Nomerotski⁵⁴, A. Novoselov³⁴,
 A. Oblakowska-Mucha²⁶, V. Obraztsov³⁴, S. Oggero⁴⁰, S. Ogilvy⁵⁰, O. Okhrimenko⁴³,
 R. Oldeman^{15,d}, M. Orlandea²⁸, J.M. Otalora Goicochea², P. Owen⁵², A. Oyanguren³⁵,
 B.K. Pal⁵⁸, A. Palano^{13,b}, M. Palutan¹⁸, J. Panman³⁷, A. Papanestis⁴⁸, M. Pappagallo⁵⁰,
 C. Parkes⁵³, C.J. Parkinson⁵², G. Passaleva¹⁷, G.D. Patel⁵¹, M. Patel⁵², G.N. Patrick⁴⁸,
 C. Patrignani^{19,i}, C. Pavel-Nicorescu²⁸, A. Pazos Alvarez³⁶, A. Pearce⁵³, A. Pellegrino⁴⁰,
 G. Penso^{24,l}, M. Pepe Altarelli³⁷, S. Perazzini^{14,c}, E. Perez Trigo³⁶, A. Pérez-Calero Yzquierdo³⁵,
 P. Perret⁵, M. Perrin-Terrin⁶, L. Pescatore⁴⁴, E. Pesen⁶¹, G. Pessina²⁰, K. Petridis⁵²,
 A. Petrolini^{19,i}, A. Phan⁵⁸, E. Picatoste Olloqui³⁵, B. Pietrzyk⁴, T. Pilar⁴⁷, D. Pinci²⁴,
 S. Playfer⁴⁹, M. Plo Casasus³⁶, F. Polci⁸, G. Polok²⁵, A. Poluektov^{47,33}, E. Polcarpo²,
 A. Popov³⁴, D. Popov¹⁰, B. Popovici²⁸, C. Potterat³⁵, A. Powell⁵⁴, J. Prisciandaro³⁸,
 A. Pritchard⁵¹, C. Prouve⁷, V. Pugatch⁴³, A. Puig Navarro³⁸, G. Punzi^{22,r}, W. Qian⁴,
 B. Rachwal²⁵, J.H. Rademacker⁴⁵, B. Rakotomiamanana³⁸, M.S. Rangel², I. Raniuk⁴²,
 N. Rauschmayr³⁷, G. Raven⁴¹, S. Redford⁵⁴, S. Reichert⁵³, M.M. Reid⁴⁷, A.C. dos Reis¹,
 S. Ricciardi⁴⁸, A. Richards⁵², K. Rinnert⁵¹, V. Rives Molina³⁵, D.A. Roa Romero⁵, P. Robbe⁷,
 D.A. Roberts⁵⁷, A.B. Rodrigues¹, E. Rodrigues⁵³, P. Rodriguez Perez³⁶, S. Roiser³⁷,
 V. Romanovsky³⁴, A. Romero Vidal³⁶, M. Rotondo²¹, J. Rouvinet³⁸, T. Ruf³⁷, F. Ruffini²²,
 H. Ruiz³⁵, P. Ruiz Valls³⁵, G. Sabatino^{24,k}, J.J. Saborido Silva³⁶, N. Sagidova²⁹, P. Sail⁵⁰,
 B. Saitta^{15,d}, V. Salustino Guimaraes², B. Sanmartin Sedes³⁶, R. Santacesaria²⁴,
 C. Santamarina Rios³⁶, E. Santovetti^{23,k}, M. Sapunov⁶, A. Sarti¹⁸, C. Satriano^{24,m}, A. Satta²³,
 M. Savrie^{16,e}, D. Savrina^{30,31}, M. Schiller⁴¹, H. Schindler³⁷, M. Schlupp⁹, M. Schmelling¹⁰,
 B. Schmidt³⁷, O. Schneider³⁸, A. Schopper³⁷, M.-H. Schune⁷, R. Schwemmer³⁷, B. Sciascia¹⁸,
 A. Sciubba²⁴, M. Seco³⁶, A. Semennikov³⁰, K. Senderowska²⁶, I. Sepp⁵², N. Serra³⁹, J. Serrano⁶,
 P. Seyfert¹¹, M. Shapkin³⁴, I. Shapoval^{16,42,e}, P. Shatalov³⁰, Y. Shcheglov²⁹, T. Shears⁵¹,
 L. Shekhtman³³, O. Shevchenko⁴², V. Shevchenko³⁰, A. Shires⁹, R. Silva Coutinho⁴⁷,

M. Sirendi⁴⁶, N. Skidmore⁴⁵, T. Skwarnicki⁵⁸, N.A. Smith⁵¹, E. Smith^{54,48}, E. Smith⁵², J. Smith⁴⁶, M. Smith⁵³, M.D. Sokoloff⁵⁶, F.J.P. Soler⁵⁰, F. Soomro³⁸, D. Souza⁴⁵, B. Souza De Paula², B. Spaan⁹, A. Sparkes⁴⁹, P. Spradlin⁵⁰, F. Stagni³⁷, S. Stahl¹¹, O. Steinkamp³⁹, S. Stevenson⁵⁴, S. Stoica²⁸, S. Stone⁵⁸, B. Storaci³⁹, M. Straticiu²⁸, U. Straumann³⁹, V.K. Subbiah³⁷, L. Sun⁵⁶, W. Sutcliffe⁵², S. Swientek⁹, V. Syropoulos⁴¹, M. Szczekowski²⁷, P. Szczypka^{38,37}, D. Szilard², T. Szumlak²⁶, S. T'Jampens⁴, M. Teklishyn⁷, E. Teodorescu²⁸, F. Teubert³⁷, C. Thomas⁵⁴, E. Thomas³⁷, J. van Tilburg¹¹, V. Tisserand⁴, M. Tobin³⁸, S. Tolk⁴¹, D. Tonelli³⁷, S. Topp-Joergensen⁵⁴, N. Torr⁵⁴, E. Tournefier^{4,52}, S. Tourneur³⁸, M.T. Tran³⁸, M. Tresch³⁹, A. Tsaregorodtsev⁶, P. Tsopelas⁴⁰, N. Tuning^{40,37}, M. Ubeda Garcia³⁷, A. Ukleja²⁷, A. Ustyuzhanin^{52,p}, U. Uwer¹¹, V. Vagnoni¹⁴, G. Valenti¹⁴, A. Vallier⁷, R. Vazquez Gomez¹⁸, P. Vazquez Regueiro³⁶, C. Vázquez Sierra³⁶, S. Vecchi¹⁶, J.J. Velthuis⁴⁵, M. Veltri^{17,g}, G. Veneziano³⁸, M. Vesterinen³⁷, B. Viaud⁷, D. Vieira², X. Vilasis-Cardona^{35,n}, A. Vollhardt³⁹, D. Volyanskyy¹⁰, D. Voong⁴⁵, A. Vorobyev²⁹, V. Vorobyev³³, C. Voß⁶⁰, H. Voss¹⁰, R. Waldi⁶⁰, C. Wallace⁴⁷, R. Wallace¹², S. Wandernoth¹¹, J. Wang⁵⁸, D.R. Ward⁴⁶, N.K. Watson⁴⁴, A.D. Webber⁵³, D. Websdale⁵², M. Whitehead⁴⁷, J. Wicht³⁷, J. Wiechczynski²⁵, D. Wiedner¹¹, L. Wiggers⁴⁰, G. Wilkinson⁵⁴, M.P. Williams^{47,48}, M. Williams⁵⁵, F.F. Wilson⁴⁸, J. Wimberley⁵⁷, J. Wishahi⁹, W. Wislicki²⁷, M. Witek²⁵, G. Wormser⁷, S.A. Wotton⁴⁶, S. Wright⁴⁶, S. Wu³, K. Wyllie³⁷, Y. Xie^{49,37}, Z. Xing⁵⁸, Z. Yang³, X. Yuan³, O. Yushchenko³⁴, M. Zangoli¹⁴, M. Zavertyaev^{10,a}, F. Zhang³, L. Zhang⁵⁸, W.C. Zhang¹², Y. Zhang³, A. Zhelezov¹¹, A. Zhokhov³⁰, L. Zhong³, A. Zvyagin³⁷.

¹ Centro Brasileiro de Pesquisas Físicas (CBPF), Rio de Janeiro, Brazil

² Universidade Federal do Rio de Janeiro (UFRJ), Rio de Janeiro, Brazil

³ Center for High Energy Physics, Tsinghua University, Beijing, China

⁴ LAPP, Université de Savoie, CNRS/IN2P3, Annecy-Le-Vieux, France

⁵ Clermont Université, Université Blaise Pascal, CNRS/IN2P3, LPC, Clermont-Ferrand, France

⁶ CPPM, Aix-Marseille Université, CNRS/IN2P3, Marseille, France

⁷ LAL, Université Paris-Sud, CNRS/IN2P3, Orsay, France

⁸ LPNHE, Université Pierre et Marie Curie, Université Paris Diderot, CNRS/IN2P3, Paris, France

⁹ Fakultät Physik, Technische Universität Dortmund, Dortmund, Germany

¹⁰ Max-Planck-Institut für Kernphysik (MPIK), Heidelberg, Germany

¹¹ Physikalisches Institut, Ruprecht-Karls-Universität Heidelberg, Heidelberg, Germany

¹² School of Physics, University College Dublin, Dublin, Ireland

¹³ Sezione INFN di Bari, Bari, Italy

¹⁴ Sezione INFN di Bologna, Bologna, Italy

¹⁵ Sezione INFN di Cagliari, Cagliari, Italy

¹⁶ Sezione INFN di Ferrara, Ferrara, Italy

¹⁷ Sezione INFN di Firenze, Firenze, Italy

¹⁸ Laboratori Nazionali dell'INFN di Frascati, Frascati, Italy

¹⁹ Sezione INFN di Genova, Genova, Italy

²⁰ Sezione INFN di Milano Bicocca, Milano, Italy

²¹ Sezione INFN di Padova, Padova, Italy

²² Sezione INFN di Pisa, Pisa, Italy

²³ Sezione INFN di Roma Tor Vergata, Roma, Italy

²⁴ Sezione INFN di Roma La Sapienza, Roma, Italy

²⁵ Henryk Niewodniczanski Institute of Nuclear Physics Polish Academy of Sciences, Kraków, Poland

²⁶ AGH - University of Science and Technology, Faculty of Physics and Applied Computer Science, Kraków, Poland

²⁷ National Center for Nuclear Research (NCBJ), Warsaw, Poland

- ²⁸ Horia Hulubei National Institute of Physics and Nuclear Engineering, Bucharest-Magurele, Romania
- ²⁹ Petersburg Nuclear Physics Institute (PNPI), Gatchina, Russia
- ³⁰ Institute of Theoretical and Experimental Physics (ITEP), Moscow, Russia
- ³¹ Institute of Nuclear Physics, Moscow State University (SINP MSU), Moscow, Russia
- ³² Institute for Nuclear Research of the Russian Academy of Sciences (INR RAN), Moscow, Russia
- ³³ Budker Institute of Nuclear Physics (SB RAS) and Novosibirsk State University, Novosibirsk, Russia
- ³⁴ Institute for High Energy Physics (IHEP), Protvino, Russia
- ³⁵ Universitat de Barcelona, Barcelona, Spain
- ³⁶ Universidad de Santiago de Compostela, Santiago de Compostela, Spain
- ³⁷ European Organization for Nuclear Research (CERN), Geneva, Switzerland
- ³⁸ Ecole Polytechnique Fédérale de Lausanne (EPFL), Lausanne, Switzerland
- ³⁹ Physik-Institut, Universität Zürich, Zürich, Switzerland
- ⁴⁰ Nikhef National Institute for Subatomic Physics, Amsterdam, The Netherlands
- ⁴¹ Nikhef National Institute for Subatomic Physics and VU University Amsterdam, Amsterdam, The Netherlands
- ⁴² NSC Kharkiv Institute of Physics and Technology (NSC KIPT), Kharkiv, Ukraine
- ⁴³ Institute for Nuclear Research of the National Academy of Sciences (KINR), Kyiv, Ukraine
- ⁴⁴ University of Birmingham, Birmingham, United Kingdom
- ⁴⁵ H.H. Wills Physics Laboratory, University of Bristol, Bristol, United Kingdom
- ⁴⁶ Cavendish Laboratory, University of Cambridge, Cambridge, United Kingdom
- ⁴⁷ Department of Physics, University of Warwick, Coventry, United Kingdom
- ⁴⁸ STFC Rutherford Appleton Laboratory, Didcot, United Kingdom
- ⁴⁹ School of Physics and Astronomy, University of Edinburgh, Edinburgh, United Kingdom
- ⁵⁰ School of Physics and Astronomy, University of Glasgow, Glasgow, United Kingdom
- ⁵¹ Oliver Lodge Laboratory, University of Liverpool, Liverpool, United Kingdom
- ⁵² Imperial College London, London, United Kingdom
- ⁵³ School of Physics and Astronomy, University of Manchester, Manchester, United Kingdom
- ⁵⁴ Department of Physics, University of Oxford, Oxford, United Kingdom
- ⁵⁵ Massachusetts Institute of Technology, Cambridge, MA, United States
- ⁵⁶ University of Cincinnati, Cincinnati, OH, United States
- ⁵⁷ University of Maryland, College Park, MD, United States
- ⁵⁸ Syracuse University, Syracuse, NY, United States
- ⁵⁹ Pontifícia Universidade Católica do Rio de Janeiro (PUC-Rio), Rio de Janeiro, Brazil, associated to ²
- ⁶⁰ Institut für Physik, Universität Rostock, Rostock, Germany, associated to ¹¹
- ⁶¹ Celal Bayar University, Manisa, Turkey, associated to ³⁷

^a P.N. Lebedev Physical Institute, Russian Academy of Science (LPI RAS), Moscow, Russia

^b Università di Bari, Bari, Italy

^c Università di Bologna, Bologna, Italy

^d Università di Cagliari, Cagliari, Italy

^e Università di Ferrara, Ferrara, Italy

^f Università di Firenze, Firenze, Italy

^g Università di Urbino, Urbino, Italy

^h Università di Modena e Reggio Emilia, Modena, Italy

ⁱ Università di Genova, Genova, Italy

^j Università di Milano Bicocca, Milano, Italy

^k Università di Roma Tor Vergata, Roma, Italy

^l Università di Roma La Sapienza, Roma, Italy

^m Università della Basilicata, Potenza, Italy

ⁿ LIFAELS, La Salle, Universitat Ramon Llull, Barcelona, Spain

^o Hanoi University of Science, Hanoi, Viet Nam

^p Institute of Physics and Technology, Moscow, Russia

^q*Università di Padova, Padova, Italy*

^r*Università di Pisa, Pisa, Italy*

^s*Scuola Normale Superiore, Pisa, Italy*

1 Introduction

The suppression of heavy quarkonia production [1] is one of the most distinctive signatures of the formation of quark-gluon plasma, a hot nuclear medium created in ultrarelativistic heavy-ion collisions. However, the suppression of heavy quarkonia and light hadron production can also take place in proton-nucleus (pA) collisions, where the quark-gluon plasma cannot be created and only cold nuclear matter effects, such as nuclear absorption, shadowing and parton energy loss in initial and final states occur [2–9]. The study of pA collisions is important to disentangle the effects of quark-gluon plasma from cold nuclear matter, and to provide essential input to the understanding of nucleus-nucleus collisions. Nuclear effects are usually characterized by the nuclear modification factor, defined as the production cross-section of a given particle per nucleon in pA collisions divided by that in proton-proton (pp) collisions [4],

$$R_{pA}(y, \sqrt{s_{NN}}) \equiv \frac{1}{A} \frac{d\sigma_{pA}(y, \sqrt{s_{NN}})/dy}{d\sigma_{pp}(y, \sqrt{s_{NN}})/dy}, \quad (1)$$

where A is the atomic mass number of the nucleus, y is the rapidity of the particle in the proton-nucleon centre-of-mass frame, and $\sqrt{s_{NN}}$ is the centre-of-mass energy. The suppression of heavy quarkonia and light hadrons at large rapidity has been observed in pA collisions [10, 11] and in deuteron-gold collisions [12–14], but has not been studied in proton-lead (pPb) collisions at the TeV scale. Previous experiments [10–14] have also shown evidence that the J/ψ production cross-section in the forward region (positive rapidity) of pA collisions differs from that in the backward region (negative rapidity), where “forward” and “backward” are defined relative to the direction of the proton beam. Measurements of the nuclear modification factor R_{pPb} and the forward-backward production ratio

$$R_{FB}(y, \sqrt{s_{NN}}) \equiv \frac{R_{pPb}(+|y|, \sqrt{s_{NN}})}{R_{pPb}(-|y|, \sqrt{s_{NN}})} \quad (2)$$

are sensitive to cold nuclear matter effects. The advantage of measuring the ratio R_{FB} is that it does not rely on the knowledge of the J/ψ production cross-section in pp collisions.

The asymmetric layout of the LHCb experiment [15], covering the pseudorapidity range $2 < \eta < 5$, allows a measurement of R_{pPb} for both the forward and backward regions, taking advantage of the inversion of the proton and lead beams during the pPb data-taking period in 2013. The energy of the proton beam is 4 TeV, while that of the lead beam is 1.58 TeV per nucleon, resulting in a centre-of-mass energy of the proton-nucleon system of 5.02 TeV, approximated as $\sqrt{s_{NN}} = 5$ TeV due to the uncertainty of the beam energy. Since the energy per nucleon in the proton beam is significantly larger than that in the lead beam, the proton-nucleon centre-of-mass system has a rapidity in the laboratory frame of +0.47 (−0.47) for pPb forward (backward) collisions. This results in a shift of the rapidity coverage in the proton-nucleon centre-of-mass system, ranging from about 1.5 to 4.0 for forward pPb collisions and from −5.0 to −2.5 for backward pPb collisions. The excellent vertexing capability of LHCb allows a separation of prompt J/ψ mesons,

which originate directly from the proton-nucleon collision, and J/ψ mesons from b -hadron decays (abbreviated as “ J/ψ from b ” in the following). The sum of these two components is referred to as inclusive J/ψ mesons.

In this paper, the differential production cross-sections of prompt J/ψ mesons and J/ψ from b are measured for the first time in $p\text{Pb}$ collisions at $\sqrt{s_{NN}} = 5$ TeV. Measurements of $R_{p\text{Pb}}$ and R_{FB} , for both prompt J/ψ mesons and J/ψ from b , are presented. For the ease of the comparison with other experiments, results for inclusive J/ψ mesons are also given.

2 Detector and data set

The LHCb detector [15] is a single-arm forward spectrometer designed for the study of particles containing b or c quarks. The detector includes a high precision tracking system consisting of a silicon-strip vertex detector (VELO) surrounding the pp interaction region, a large-area silicon-strip detector located upstream of a dipole magnet with a bending power of about 4 Tm, and three stations of silicon-strip detectors and straw drift tubes placed downstream. The VELO has the unique feature of being located very close to the beam line (about 8 mm). This allows excellent resolutions in reconstructing the position of the collision point, *i.e.*, the primary vertex, and the vertex of the hadron decay, *i.e.*, the secondary vertex. For primary (secondary) vertices, the resolution in the plane transverse to the beam is $\sigma_{x(y)} \approx 10$ (20) μm , and that along the beam is $\sigma_z \approx 50$ (200) μm . The combined tracking system has a momentum resolution $\Delta p/p$ that varies from 0.4% at 5 GeV/ c to 0.6% at 100 GeV/ c , and an impact parameter resolution of 20 μm for tracks with large transverse momentum. Charged hadrons are identified using two ring-imaging Cherenkov detectors [16]. Photon, electron and hadron candidates are identified by a calorimeter system consisting of scintillating-pad and preshower detectors, an electromagnetic calorimeter and a hadronic calorimeter. Muons are identified by a system composed of alternating layers of iron and multiwire proportional chambers [17]. The trigger [18] consists of a hardware stage, based on information from the calorimeter and muon systems, followed by a software stage which applies a full event reconstruction.

This analysis is based on a data sample acquired during the $p\text{Pb}$ run in early 2013, corresponding to an integrated luminosity of 1.1 nb^{-1} (0.5 nb^{-1}) for forward (backward) collisions. The instantaneous luminosity was around $5 \times 10^{27} \text{cm}^{-2}\text{s}^{-1}$, five orders of magnitude below the typical LHCb luminosity for pp collisions.

The hardware trigger during this period was simply an interaction trigger, which rejects empty events. The software trigger requires one well-reconstructed track with hits in the muon system and a p_{T} greater than 600 MeV/ c .

Simulated samples based on pp collisions at 8 TeV are reweighted to reproduce the experimental data at 5 TeV, and are used to determine acceptance and reconstruction efficiencies. In the simulation, pp collisions are generated using PYTHIA 6.4 [19] with a specific LHCb configuration [20]. Hadron decays are described by EVTGEN [21], where final state radiation is generated using PHOTOS [22]. The interactions of the generated particles with the detector and its response are implemented using the GEANT4 toolkit [23] as described in Ref. [24].

3 Event selection and cross-section determination

The J/ψ production cross-section measurement follows the approach described in Refs. [25–27]. The J/ψ candidates are reconstructed and selected using dimuon final states. Reconstructed $J/\psi \rightarrow \mu^+\mu^-$ candidates are selected from pairs of oppositely charged particles with transverse momentum $p_T > 0.7 \text{ GeV}/c$, which are identified as muons by the muon detector and have a track fit χ^2 per number of degree of freedom less than 3. To suppress combinatorial background, the difference between the logarithms of the likelihoods for the muon and the pion hypotheses $\text{DLL}_{\mu\pi}$ [17, 28] is required to be greater than 1.0 (3.5) for the forward (backward) sample. The two muons are required to originate from a common vertex with a χ^2 -probability larger than 0.5%. Candidates are kept if the reconstructed invariant mass is in the range $2990 < m_{\mu\mu} < 3210 \text{ MeV}/c^2$, which is within about $\pm 110 \text{ MeV}/c^2$ of the known J/ψ mass [29].

The double differential cross-section for J/ψ production in a given (p_T, y) bin is defined as

$$\frac{d^2\sigma}{dp_T dy} = \frac{N^{\text{cor}}(J/\psi \rightarrow \mu^+\mu^-)}{\mathcal{L} \times \mathcal{B}(J/\psi \rightarrow \mu^+\mu^-) \times \Delta p_T \times \Delta y}, \quad (3)$$

where $N^{\text{cor}}(J/\psi \rightarrow \mu^+\mu^-)$ is the efficiency-corrected number of observed $J/\psi \rightarrow \mu^+\mu^-$ signal candidates in the given bin, \mathcal{L} is the integrated luminosity, $\mathcal{B}(J/\psi \rightarrow \mu^+\mu^-) = (5.93 \pm 0.06)\%$ [29] is the branching fraction of the $J/\psi \rightarrow \mu^+\mu^-$ decay, and Δp_T and Δy the widths of the (p_T, y) bin.

The numbers of prompt J/ψ mesons and J/ψ from b in bins of the kinematic variables y and p_T are obtained by performing combined extended maximum likelihood fits to the unbinned distributions of dimuon mass and pseudo proper time t_z in each kinematic bin. The pseudo proper time of the J/ψ meson is defined as

$$t_z = \frac{(z_{J/\psi} - z_{\text{PV}}) \times M_{J/\psi}}{p_z}, \quad (4)$$

where $z_{J/\psi}$ is the z position of the J/ψ decay vertex, z_{PV} that of the primary vertex, p_z is the z component of the measured J/ψ momentum, and $M_{J/\psi}$ is the known J/ψ mass [29].

The signal dimuon invariant mass distribution in each p_T and y bin is modelled with a Crystal Ball function [30], and the combinatorial background with an exponential function. The t_z signal distribution is described by the sum of a δ -function at $t_z = 0$ for prompt J/ψ production and an exponential decay function for J/ψ from b , both convolved with a double-Gaussian resolution function whose parameters are free in the fit. The t_z distribution of background in each kinematic bin is independently modelled with an empirical function based on the t_z distribution observed in background events obtained using the *sPlot* technique [31]. All the parameters of the t_z background distribution are fixed in the final combined fits to the distributions of invariant mass and pseudo proper time. The total fit function is the sum of the products of the mass and t_z fit functions for the signal and background components.

Figure 1 shows projections of the fit to the dimuon invariant mass and t_z distributions, for two representative bins of y in the forward and backward regions. The dimuon invariant

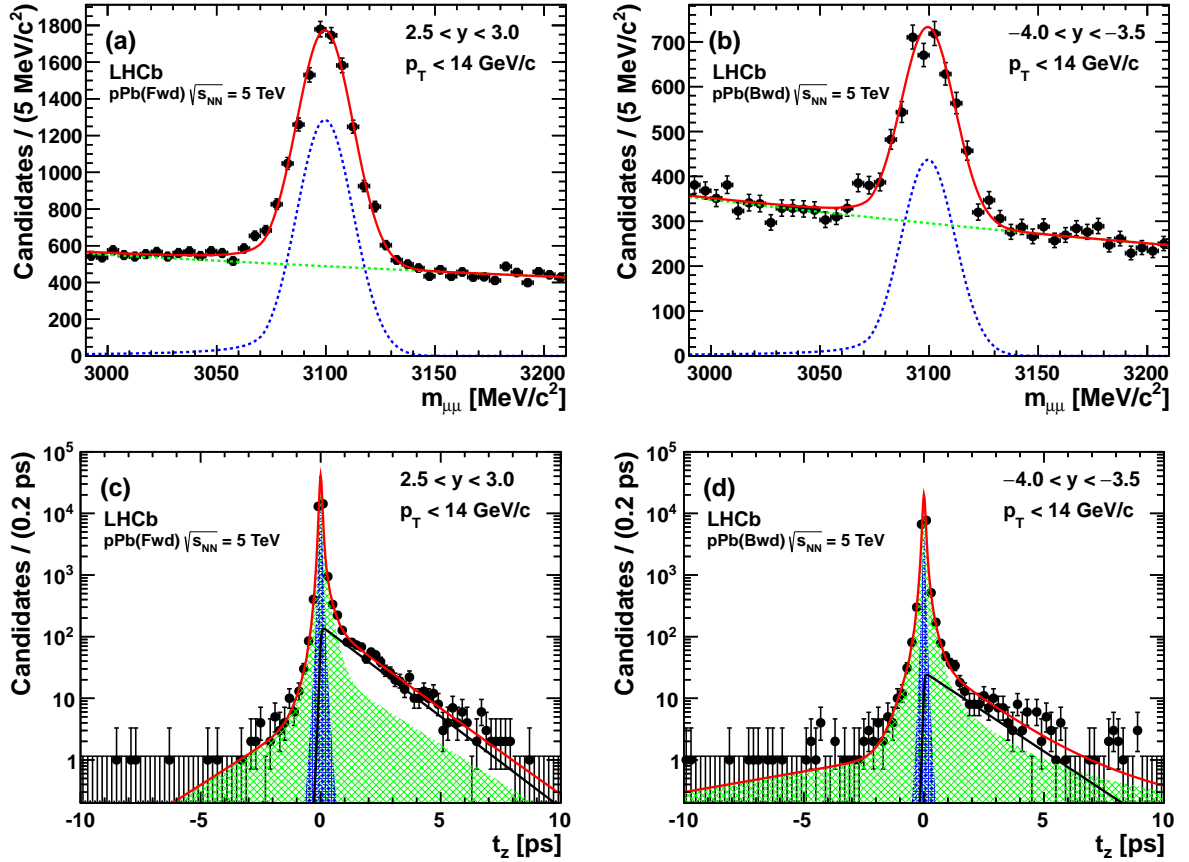


Figure 1: Projections of the combined fit on (a, b) dimuon invariant mass and (c, d) t_z in two representative bins in the (a, c) forward and (b, d) backward samples. For the mass projections the (red solid curve) total fitted function is shown together with the (blue dotted curve) J/ψ signal and (green dotted curve) background contributions. For the t_z projections the total fitted function is indicated by the solid red curve, the background by the green hatched area, the prompt signal by the blue area and J/ψ from b by the solid black curve.

mass resolution is about $15 \text{ MeV}/c^2$ for both the forward and backward samples, consistent with the mass resolution measured in pp collisions [25–27] and in simulation. The total signal yield for prompt J/ψ mesons in the forward (backward) sample is $25\,280 \pm 240$ ($8\,830 \pm 160$); the total signal yield for J/ψ from b in the forward (backward) sample is $3\,720 \pm 80$ (890 ± 40). Based on the fit results for prompt J/ψ mesons and J/ψ from b , a signal weight factor w_i for the i th candidate is obtained with the *sPlot* technique, using the dimuon invariant mass and t_z as control variables. The sum of w_i/ε_i over all events in a given bin leads to the efficiency-corrected signal yield N^{cor} in that bin, where the efficiency ε_i depends on p_T and y and includes the geometric acceptance, reconstruction, muon identification, and trigger efficiencies.

The acceptance and reconstruction efficiencies are estimated from simulated samples, assuming production of unpolarized J/ψ mesons. The efficiency of the $\text{DLL}_{\mu\pi}$ selection is

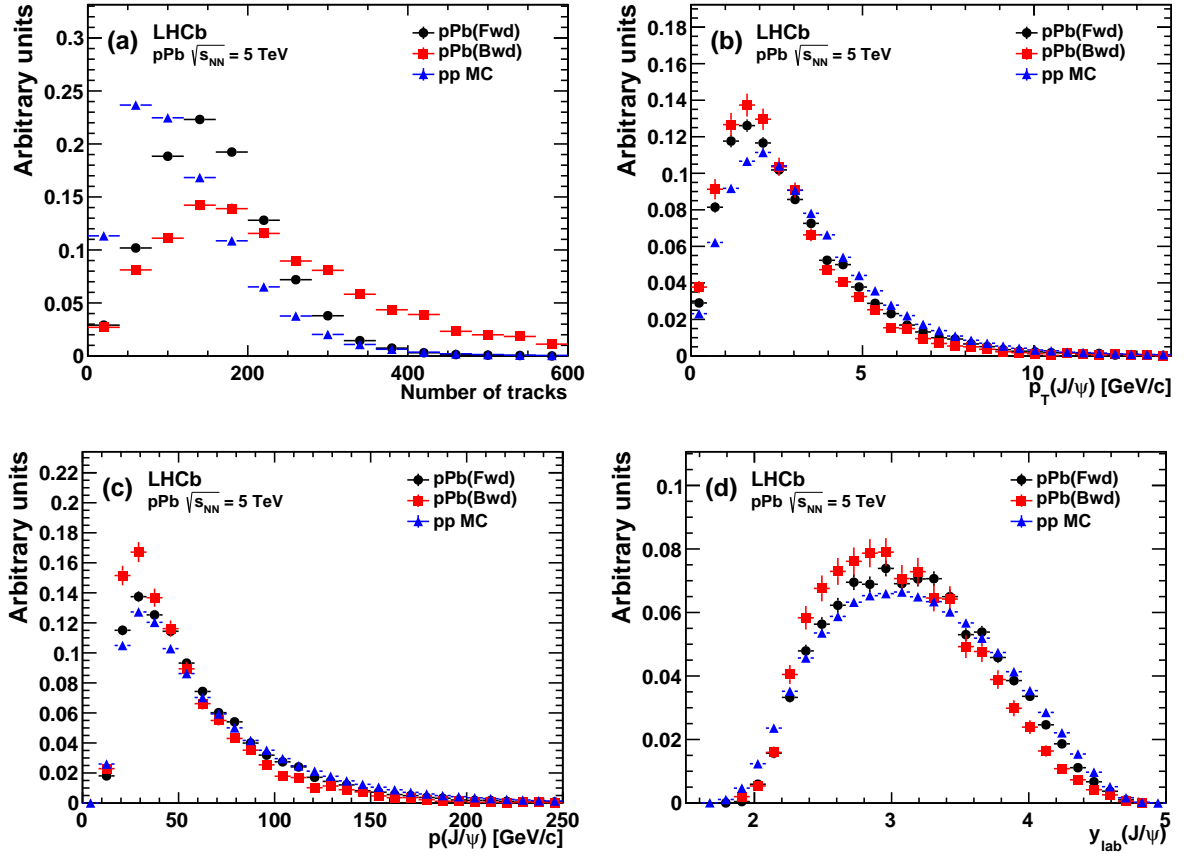


Figure 2: Normalized distributions of (a) track multiplicity and the J/ψ (b) transverse momentum p_T , (c) momentum p , and (d) rapidity in laboratory frame y_{lab} in (black dots) forward and (red squares) backward regions of pPb collisions, and in (blue triangles) simulated pp collisions. The distributions are background subtracted using the *sPlot* technique.

obtained by a data-driven tag-and-probe approach [32]. The trigger efficiency is obtained from data using a sample of J/ψ decays unbiased by the trigger decision [18].

Figure 2 shows the background-subtracted distributions of the track multiplicity per event and the J/ψ p_T , p , and the rapidity in the laboratory frame y_{lab} in experimental pPb and simulated pp data. The differences in the distributions of p_T , p , and y_{lab} between data and simulated samples are small. Sizeable differences in the distributions of the track multiplicity are observed, particularly between the simulation and the backward sample, for which the particle production cross-section is larger [10, 12–14]. To take this effect into account, the simulated pp samples are reweighted to match the data with weight factors derived from the distributions in Fig. 2.

Table 1: Relative systematic uncertainties on the differential production cross-section.

Source	Forward (%)	Backward (%)
<i>Correlated between bins</i>		
Mass fits	2.3	3.4
Radiative tail	1.0	1.0
Muon identification	1.3	1.3
Tracking efficiency	1.5	1.5
Luminosity	3.0	3.0
$\mathcal{B}(J/\psi \rightarrow \mu^+ \mu^-)$	1.0	1.0
<i>Uncorrelated between bins</i>		
Binning	0.1 – 8.7	0.1 – 6.1
Multiplicity weight	0.1 – 3.0	0.2 – 4.3
t_z fit (<i>only for J/ψ from b</i>)	0.2 – 12	0.2 – 13

4 Systematic uncertainties

Acceptance and reconstruction efficiencies depend not only on the kinematic distributions of the J/ψ meson but also on its polarisation. The LHCb measurement in pp collisions [33] indicated a longitudinal polarization consistent with zero in most of the kinematic region. Based on the expectation that the nuclear environment does not enhance the polarisation, it is assumed that the J/ψ mesons are produced with no polarisation. No systematic uncertainty is assigned to the effect of polarisation in this analysis.

Several contributions to the systematic uncertainties affecting the cross-section measurement are discussed in the following and summarised in Table 1. The influence of the model assumed to describe the shape of the dimuon invariant mass distribution is estimated by adding a second Crystal Ball to the fit function. The relative difference of 2.3% (3.4%) in the signal yield for forward (backward) collisions is taken as a systematic uncertainty. Due to the muon bremsstrahlung, a small fraction of signal candidates with low reconstructed invariant mass are excluded from the signal mass region. This effect is included in the reconstruction efficiency, and an uncertainty of 1% is assigned based on the comparison between the observed radiative tail in data and simulation.

The systematic uncertainties due to the muon identification efficiency and the track reconstruction efficiency are estimated using a data-driven tag-and-probe method [32] based on partially reconstructed J/ψ decays. To estimate the uncertainty due to the muon identification efficiency, J/ψ candidates are reconstructed with one muon identified by the muon system (“tag”) and the other (“probe”) identified by selecting a track depositing the energy of a minimum-ionising particle in the calorimeters. The resulting uncertainty is 1.3%. Taking into account the effect of the track-multiplicity difference between $p\text{Pb}$ and pp data, an uncertainty of 1.5% is assigned due to the track reconstruction efficiency.

The luminosity is determined with an uncertainty of 3%, dominated by the differences

in the results obtained with van der Meer scans [34, 35] using the core and off-core parts of the proton beam. The uncertainty of the branching fraction of the $J/\psi \rightarrow \mu^+\mu^-$ decay is 1% [29].

Differences of the p_T and y spectra between data and simulation within a given (p_T, y) bin due to the finite bin sizes can affect the result. This effect is estimated by doubling the number of bins in p_T and shifting each rapidity bin by half a unit. The relative difference with respect to the default binning, which varies between 0.1% and 8.7% depending on the bin, is taken as systematic uncertainty. The uncertainties in most bins are below 2%, but increase in the lowest rapidity bins.

To estimate the effect of reweighting the track multiplicity in the simulation, the efficiency without reweighting is calculated. The relative difference in each bin between the two methods is taken as systematic uncertainty.

Uncertainties related to the t_z fit procedure are measured by fitting directly the t_z signal component, which is determined using the *sPlot* technique. This gives results consistent with those obtained from the combined fit; the relative difference between results in each bin is taken as systematic uncertainty.

5 Results

Single differential production cross-sections as functions of p_T and y , for both prompt J/ψ mesons and J/ψ from b in the pPb forward and backward regions, are displayed in Fig. 3 and shown in Tables 2 and 3, respectively, assuming no J/ψ polarisation.

Due to the large samples of pPb forward collisions, the double differential production cross-sections can also be measured. These results are shown in Fig. 4 and displayed in Table 4.

The integrated production cross-sections for prompt J/ψ mesons and J/ψ from b with $p_T < 14 \text{ GeV}/c$ in the forward and backward regions are measured to be

$$\begin{aligned}\sigma_F(\text{prompt } J/\psi, +1.5 < y < +4.0) &= 1168 \pm 15 \pm 60 \text{ } \mu\text{b}, \\ \sigma_B(\text{prompt } J/\psi, -2.5 < y < -5.0) &= 1293 \pm 42 \pm 82 \text{ } \mu\text{b}, \\ \sigma_F(J/\psi \text{ from } b, +1.5 < y < +4.0) &= 166.0 \pm 4.1 \pm 9.2 \text{ } \mu\text{b}, \\ \sigma_B(J/\psi \text{ from } b, -2.5 < y < -5.0) &= 118.2 \pm 6.8 \pm 12.2 \text{ } \mu\text{b},\end{aligned}$$

where the first uncertainty is statistical and the second is systematic.

The J/ψ production cross-section in pp collisions at 5 TeV, used as a reference to determine the nuclear modification factor R_{pPb} , is obtained by a power-law interpolation, $\sigma(\sqrt{s}) = (\sqrt{s}/p_0)^{p_1} \text{ } \mu\text{b}$, of previous LHCb measurements performed at 2.76, 7, and 8 TeV [25–27]. For $\sqrt{s} = 7$ and 8 TeV, measurements in the kinematic region $p_T < 14 \text{ GeV}/c$ and $2.5 < |y| < 4.0$, the common rapidity range of the forward and backward regions in the proton-nucleon centre-of-mass frame, are available. The measurements at $\sqrt{s} = 2.76 \text{ TeV}$ are rescaled to this range. The fits give $p_0 = 0.67 \pm 0.11 \text{ TeV}$ and $p_1 = 0.49 \pm 0.21$ for prompt J/ψ mesons, and $p_0 = 1.1 \pm 0.2 \text{ TeV}$ and $p_1 = 9.4 \pm 0.7$ for J/ψ from b . Alternative

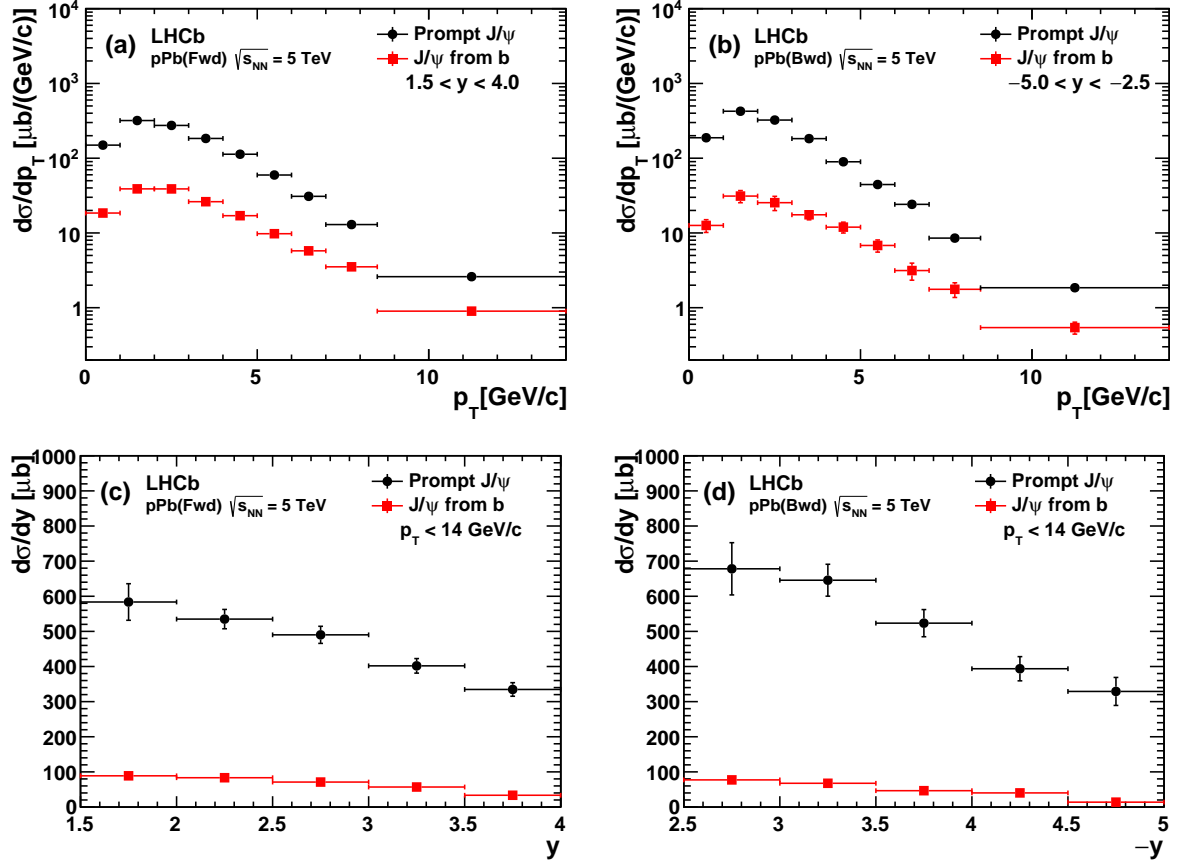


Figure 3: Single differential production cross-sections for (black dots) prompt J/ψ and (red squares) J/ψ from b as functions of (a, b) p_T and (c, d) y in the (a, c) forward and (b, d) backward regions.

interpolations based on linear and exponential fits are also tried; the largest deviation from the default value is taken as a systematic uncertainty due to the interpolation, 3.1% (3.3%) for prompt (from b) J/ψ mesons. The reference production cross-section in pp collisions at 5 TeV for prompt J/ψ mesons is $4.78 \pm 0.23 \pm 0.15$ μb , and that for J/ψ from b is $0.50 \pm 0.05 \pm 0.01$ μb . The nuclear modification factor $R_{p\text{Pb}}$ is then determined in the rapidity ranges $-4.0 < y < -2.5$ and $2.5 < y < 4.0$ for both prompt J/ψ mesons and J/ψ from b . Figure 5(a) shows the nuclear modification factor for prompt J/ψ production, together with several theoretical predictions [2–4]. The uncertainties for the theoretical predictions are obtained by taking into account minimum and maximum nuclear shadowing effects. A suppression of about 40% at large rapidity is observed for prompt J/ψ production. The measurements agree with most predictions. However, the calculation with the EPS09 NLO nuclear parton distribution function (nPDF) parameterisation [3] provides a poorer description of the measurement in the forward region. Figure 5(b) shows the nuclear modification factor for J/ψ from b , together with the theoretical predictions [2]. The data prefer a modest suppression of J/ψ from b in the forward region. This is the first indication

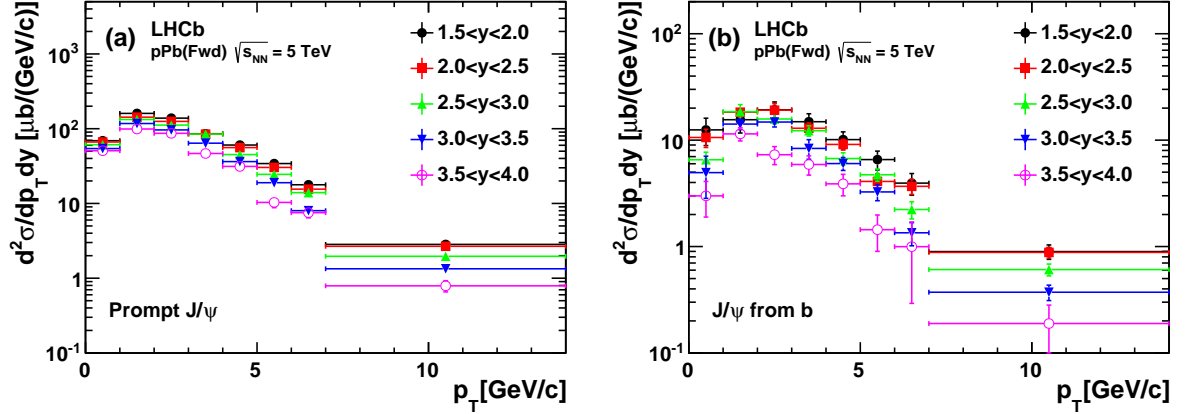


Figure 4: Double differential production cross-sections for (a) prompt J/ψ mesons and (b) J/ψ from b in the forward samples.

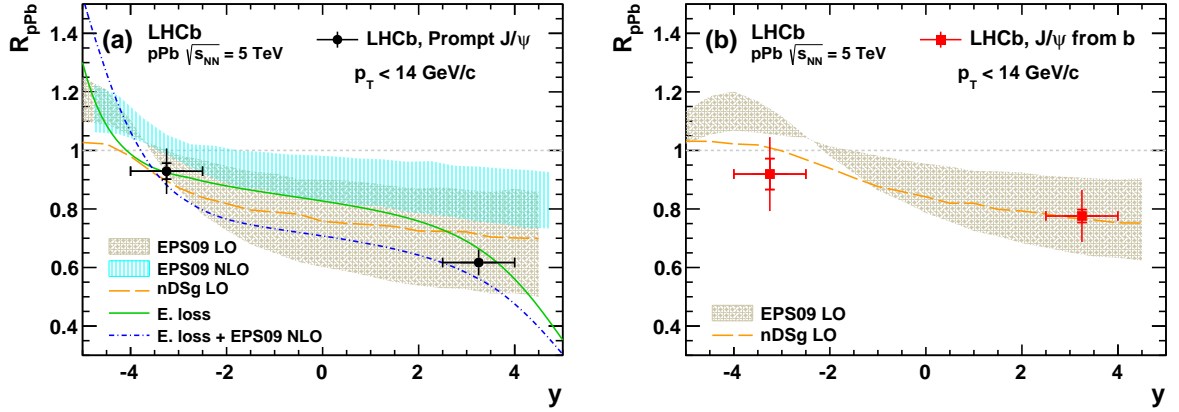


Figure 5: Nuclear modification factor R_{pPb} as a function of y for (a) prompt J/ψ mesons and (b) J/ψ from b , together with the theoretical predictions [2–4]. The inner error bars (delimited by the horizontal lines) show the statistical uncertainties; the outer ones show the statistical and systematic uncertainties added in quadrature.

of the suppression of b hadron production in pPb collisions. The theoretical predictions agree with the measurement in the forward region. In the backward region the agreement is not as good. The measured values of the nuclear modification factor, together with the results for inclusive J/ψ mesons, are given in Table 5.

Figure 6 shows the forward-backward production ratio R_{FB} as a function of $|y|$, compared with theoretical calculations [2–4]. The value of R_{FB} for J/ψ from b is closer to unity than for prompt J/ψ mesons, indicating a smaller asymmetry in the forward-backward production. The results agree with theoretical predictions. The calculation with the EPS09 NLO nPDF [3] predicts a smaller forward-backward production asymmetry for prompt J/ψ mesons than observed. Figure 7 shows the forward-backward production ratio R_{FB} as a function of p_T for prompt J/ψ mesons and J/ψ from b in the range $2.5 < y < 4.0$ of the proton-nucleon centre-of-mass frame. Theoretical predictions [3, 5] are only available

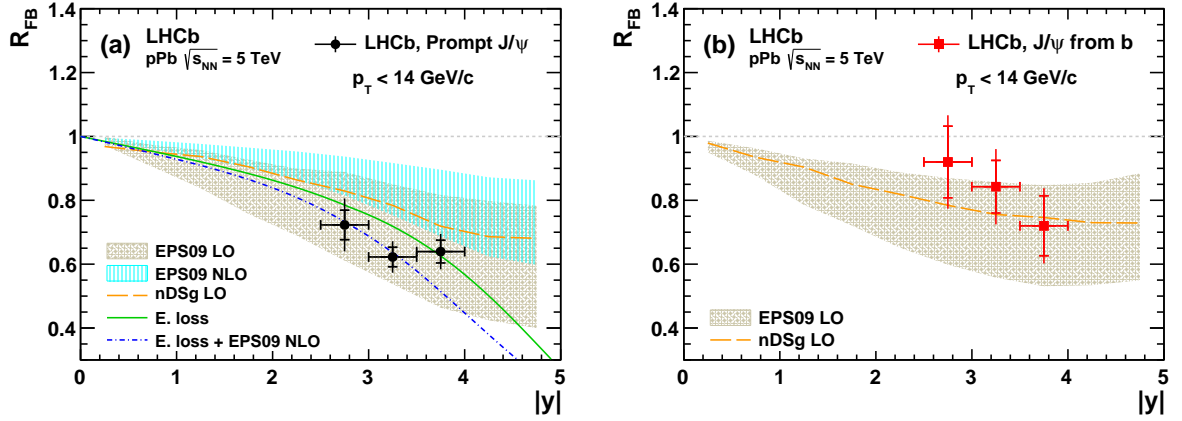


Figure 6: Forward-backward production ratio R_{FB} as a function of $|y|$ for (a) prompt J/ψ mesons and (b) J/ψ from b , together with the theoretical predictions [2–4]. The inner error bars (delimited by the horizontal lines) show the statistical uncertainties; the outer ones show the statistical and systematic uncertainties added in quadrature.

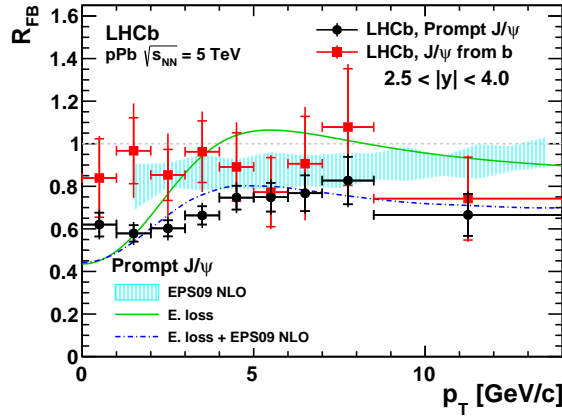


Figure 7: Forward-backward production ratio R_{FB} for (black dot) prompt J/ψ mesons and (red square) J/ψ from b as a function of p_T in the rapidity range $2.5 < |y| < 4.0$. The theoretical predictions [3, 5] are for prompt J/ψ mesons. The inner error bars (delimited by the horizontal lines) show the statistical uncertainties; the outer ones show the statistical and systematic uncertainties added in quadrature.

for prompt J/ψ mesons. The calculation [5] based on parton energy loss with the EPS09 NLO nPDF agrees with the measurement of R_{FB} for prompt J/ψ mesons. The measured values of the forward-backward production ratio R_{FB} are given in Tables 6 and 7, where the results for inclusive J/ψ mesons are also listed.

6 Conclusion

The production of prompt J/ψ mesons and those from b -hadron decays is studied in $p\text{Pb}$ collisions with the LHCb detector at the proton-nucleon centre-of-mass energy $\sqrt{s_{NN}} = 5\text{ TeV}$. The measurement is performed as a function of the transverse momentum and rapidity of the J/ψ meson in the region $p_T < 14\text{ GeV}/c$ and $1.5 < y < 4.0$ (forward) and $-5.0 < y < -2.5$ (backward). The nuclear modification factor $R_{p\text{Pb}}$ and the forward-backward production ratio R_{FB} are determined for the first time separately for prompt J/ψ mesons and those from b -hadron decays. The measurement indicates that cold nuclear matter effects are less pronounced for J/ψ mesons from b -hadron decays, hence for b hadrons, than for prompt J/ψ mesons. These results show good agreement with available theoretical predictions. The results for inclusive J/ψ mesons are in agreement with those presented by the ALICE collaboration [36].

Acknowledgements

We are grateful for useful discussions with the ALICE collaboration. We wish to thank also F. Arleo, J. P. Lansberg, and R. Vogt for stimulating and helpful suggestions. We express our gratitude to our colleagues in the CERN accelerator departments for the excellent performance of the LHC. We thank the technical and administrative staff at the LHCb institutes. We acknowledge support from CERN and from the national agencies: CAPES, CNPq, FAPERJ and FINEP (Brazil); NSFC (China); CNRS/IN2P3 and Region Auvergne (France); BMBF, DFG, HGF and MPG (Germany); SFI (Ireland); INFN (Italy); FOM and NWO (The Netherlands); SCSR (Poland); MEN/IFA (Romania); MinES, Rosatom, RFBR and NRC “Kurchatov Institute” (Russia); MinECo, XuntaGal and GENCAT (Spain); SNSF and SER (Switzerland); NAS Ukraine (Ukraine); STFC (United Kingdom); NSF (USA). We also acknowledge the support received from the ERC under FP7. The Tier1 computing centres are supported by IN2P3 (France), KIT and BMBF (Germany), INFN (Italy), NWO and SURF (The Netherlands), PIC (Spain), GridPP (United Kingdom). We are thankful for the computing resources put at our disposal by Yandex LLC (Russia), as well as to the communities behind the multiple open source software packages that we depend on.

Appendices

A Results in tables

Table 2: Single differential production cross-sections (in $\mu\text{b}/(\text{GeV}/c)$) for prompt J/ψ mesons and J/ψ from b as functions of transverse momentum. The first uncertainty is statistical, the second is the component of the systematic uncertainty that is uncorrelated between bins, and the third is the correlated component.

p_{T} [GeV/ c]	$\text{d}\sigma/\text{d}p_{\text{T}}$ (prompt J/ψ)			$\text{d}\sigma/\text{d}p_{\text{T}}$ (J/ψ from b)
Forward ($1.5 < y < 4.0$)				
0.0 – 1.0	149.6 ± 5.7	± 2.0	± 6.8	$18.5 \pm 1.6 \pm 0.9 \pm 0.8$
1.0 – 2.0	319.0 ± 11.1	± 5.3	± 14.4	$38.9 \pm 2.3 \pm 0.5 \pm 1.8$
2.0 – 3.0	274.4 ± 7.1	± 4.6	± 12.4	$38.8 \pm 2.1 \pm 0.9 \pm 1.8$
3.0 – 4.0	183.7 ± 5.1	± 3.4	± 8.3	$26.2 \pm 1.6 \pm 1.8 \pm 1.2$
4.0 – 5.0	113.0 ± 3.2	± 1.7	± 5.1	$17.0 \pm 1.1 \pm 0.2 \pm 0.8$
5.0 – 6.0	59.6 ± 2.1	± 0.7	± 2.7	$9.8 \pm 0.8 \pm 0.3 \pm 0.4$
6.0 – 7.0	30.9 ± 1.4	± 0.2	± 1.4	$5.8 \pm 0.6 \pm 0.2 \pm 0.3$
7.0 – 8.5	12.9 ± 0.6	± 0.2	± 0.6	$3.5 \pm 0.3 \pm 0.0 \pm 0.2$
8.5 – 14	2.6 ± 0.1	± 0.0	± 0.1	$0.9 \pm 0.1 \pm 0.0 \pm 0.0$
Backward ($-5.0 < y < -2.5$)				
0.0 – 1.0	187.7 ± 14.0	± 5.6	± 9.9	$12.6 \pm 2.1 \pm 1.0 \pm 0.7$
1.0 – 2.0	425.0 ± 23.6	± 7.8	± 22.4	$31.1 \pm 3.8 \pm 4.1 \pm 1.6$
2.0 – 3.0	323.9 ± 16.7	± 9.1	± 17.1	$25.4 \pm 3.0 \pm 4.4 \pm 1.3$
3.0 – 4.0	182.7 ± 9.6	± 2.2	± 9.6	$17.5 \pm 2.1 \pm 1.1 \pm 0.9$
4.0 – 5.0	89.6 ± 5.5	± 1.3	± 4.7	$12.0 \pm 1.7 \pm 0.8 \pm 0.6$
5.0 – 6.0	44.4 ± 3.1	± 1.0	± 2.3	$6.8 \pm 1.2 \pm 0.2 \pm 0.4$
6.0 – 7.0	24.1 ± 2.1	± 0.4	± 1.3	$3.1 \pm 0.7 \pm 0.4 \pm 0.2$
7.0 – 8.5	8.5 ± 0.9	± 0.3	± 0.5	$1.8 \pm 0.4 \pm 0.1 \pm 0.1$
8.5 – 14	1.9 ± 0.2	± 0.0	± 0.1	$0.5 \pm 0.1 \pm 0.0 \pm 0.0$

Table 3: Single differential production cross-sections (in μb) for prompt J/ψ mesons and J/ψ from b as functions of rapidity. The first uncertainty is statistical, the second is the component of the systematic uncertainty that is uncorrelated between bins, and the third is the correlated component.

$ y $	$d\sigma/dy$ (prompt J/ψ)			$d\sigma/dy$ (J/ψ from b)
Forward ($p_{\text{T}} < 14 \text{ GeV}/c$)				
1.5 – 2.0	583.7 ± 21.0	± 39.6	± 26.4	$88.8 \pm 5.9 \pm 6.1 \pm 4.0$
2.0 – 2.5	535.0 ± 11.8	± 5.6	± 24.2	$83.4 \pm 3.4 \pm 2.1 \pm 3.8$
2.5 – 3.0	490.2 ± 9.7	± 2.6	± 22.2	$71.0 \pm 2.8 \pm 0.4 \pm 3.2$
3.0 – 3.5	401.9 ± 8.5	± 5.2	± 18.2	$56.9 \pm 2.6 \pm 2.4 \pm 2.6$
3.5 – 4.0	334.7 ± 8.6	± 8.4	± 15.1	$33.4 \pm 2.6 \pm 2.5 \pm 1.5$
Backward ($p_{\text{T}} < 14 \text{ GeV}/c$)				
2.5 – 3.0	678.2 ± 41.8	± 50.6	± 35.6	$77.2 \pm 8.9 \pm 6.4 \pm 4.0$
3.0 – 3.5	645.7 ± 28.7	± 9.6	± 33.9	$67.5 \pm 5.8 \pm 4.7 \pm 3.5$
3.5 – 4.0	523.4 ± 25.9	± 8.0	± 27.4	$46.5 \pm 4.8 \pm 1.1 \pm 2.4$
4.0 – 4.5	393.7 ± 26.1	± 8.7	± 20.6	$40.1 \pm 5.2 \pm 4.6 \pm 2.1$
4.5 – 5.0	329.0 ± 31.3	± 15.7	± 17.3	$13.8 \pm 4.5 \pm 1.3 \pm 0.7$

Table 4: Double differential production cross-sections (in $\mu\text{b}/(\text{GeV}/c)$) for prompt J/ψ mesons and J/ψ from b as functions of p_T and y in $p\text{Pb}$ forward data. The first uncertainty is statistical, the second is the component of the systematic uncertainty that is uncorrelated between bins, and the third is the correlated component.

p_T [GeV/ c]	$1.5 < y < 2.0$			$2.0 < y < 2.5$			$2.5 < y < 3.0$			$3.0 < y < 3.5$			$3.5 < y < 4.0$		
prompt J/ψ															
0.0 – 1.0	69.1 \pm 7.7 \pm 3.7 \pm 3.1	66.3 \pm 4.5 \pm 0.7 \pm 3.0	61.1 \pm 4.0 \pm 0.8 \pm 2.8	54.2 \pm 3.3 \pm 1.9 \pm 2.5	50.7 \pm 3.3 \pm 2.3 \pm 2.3										
1.0 – 2.0	160.2 \pm 11.9 \pm 12.4 \pm 7.3	142.7 \pm 6.9 \pm 1.6 \pm 6.5	132.8 \pm 5.5 \pm 1.5 \pm 6.0	117.3 \pm 4.9 \pm 0.9 \pm 5.3	99.1 \pm 4.9 \pm 2.4 \pm 4.5										
2.0 – 3.0	138.5 \pm 9.9 \pm 10.0 \pm 6.3	125.2 \pm 5.4 \pm 1.4 \pm 5.7	111.8 \pm 4.4 \pm 0.6 \pm 5.1	96.3 \pm 4.0 \pm 1.4 \pm 4.4	86.7 \pm 4.9 \pm 4.1 \pm 3.9										
3.0 – 4.0	85.6 \pm 7.0 \pm 7.6 \pm 3.9	84.5 \pm 3.9 \pm 1.2 \pm 3.8	84.7 \pm 3.4 \pm 1.9 \pm 3.8	64.0 \pm 2.9 \pm 1.6 \pm 2.9	46.6 \pm 3.5 \pm 0.7 \pm 2.1										
4.0 – 5.0	60.4 \pm 4.5 \pm 4.0 \pm 2.7	55.9 \pm 2.6 \pm 0.9 \pm 2.5	45.1 \pm 2.0 \pm 0.9 \pm 2.0	36.3 \pm 1.9 \pm 0.4 \pm 1.6	31.3 \pm 2.4 \pm 0.6 \pm 1.4										
5.0 – 6.0	34.2 \pm 3.0 \pm 0.9 \pm 1.5	30.3 \pm 1.7 \pm 0.8 \pm 1.4	24.5 \pm 1.3 \pm 0.5 \pm 1.1	18.9 \pm 1.2 \pm 0.3 \pm 0.9	10.3 \pm 1.4 \pm 0.5 \pm 0.5										
6.0 – 7.0	17.8 \pm 1.9 \pm 0.6 \pm 0.8	15.5 \pm 1.1 \pm 0.1 \pm 0.7	14.0 \pm 0.9 \pm 0.1 \pm 0.6	8.0 \pm 0.8 \pm 0.1 \pm 0.4	7.5 \pm 1.0 \pm 0.2 \pm 0.3										
7.0 – 14	2.8 \pm 0.2 \pm 0.1 \pm 0.1	2.7 \pm 0.2 \pm 0.1 \pm 0.1	2.0 \pm 0.1 \pm 0.0 \pm 0.1	1.3 \pm 0.1 \pm 0.0 \pm 0.1	0.8 \pm 0.1 \pm 0.0 \pm 0.0										
J/ψ from b															
0.0 – 1.0	12.5 \pm 2.7 \pm 2.4 \pm 0.6	10.6 \pm 1.3 \pm 1.5 \pm 0.5	6.5 \pm 1.0 \pm 0.6 \pm 0.3	5.0 \pm 0.9 \pm 1.9 \pm 0.2	3.0 \pm 0.8 \pm 0.8 \pm 0.1										
1.0 – 2.0	15.6 \pm 2.7 \pm 2.7 \pm 0.7	18.3 \pm 1.7 \pm 0.3 \pm 0.8	18.5 \pm 1.5 \pm 2.5 \pm 0.8	14.2 \pm 1.4 \pm 0.4 \pm 0.6	11.4 \pm 1.5 \pm 0.5 \pm 0.5										
2.0 – 3.0	19.3 \pm 2.9 \pm 1.9 \pm 0.9	19.1 \pm 1.6 \pm 2.3 \pm 0.9	15.8 \pm 1.3 \pm 0.5 \pm 0.7	14.8 \pm 1.3 \pm 0.2 \pm 0.7	7.3 \pm 1.3 \pm 0.3 \pm 0.3										
3.0 – 4.0	14.9 \pm 2.4 \pm 1.3 \pm 0.7	12.9 \pm 1.3 \pm 0.7 \pm 0.6	12.3 \pm 1.1 \pm 0.6 \pm 0.6	8.4 \pm 0.9 \pm 1.4 \pm 0.4	5.9 \pm 1.1 \pm 0.3 \pm 0.3										
4.0 – 5.0	10.1 \pm 1.6 \pm 0.8 \pm 0.5	9.1 \pm 0.9 \pm 0.3 \pm 0.4	6.7 \pm 0.8 \pm 0.4 \pm 0.3	6.0 \pm 0.8 \pm 0.1 \pm 0.3	3.9 \pm 0.8 \pm 0.3 \pm 0.2										
5.0 – 6.0	6.6 \pm 1.2 \pm 0.3 \pm 0.3	4.1 \pm 0.6 \pm 0.3 \pm 0.2	4.7 \pm 0.6 \pm 0.1 \pm 0.2	3.3 \pm 0.5 \pm 0.2 \pm 0.1	1.4 \pm 0.5 \pm 0.2 \pm 0.1										
6.0 – 7.0	3.9 \pm 0.8 \pm 0.4 \pm 0.2	3.7 \pm 0.6 \pm 0.1 \pm 0.2	2.2 \pm 0.4 \pm 0.0 \pm 0.1	1.3 \pm 0.3 \pm 0.1 \pm 0.1	1.0 \pm 0.4 \pm 0.6 \pm 0.0										
7.0 – 14	0.9 \pm 0.1 \pm 0.0 \pm 0.0	0.9 \pm 0.1 \pm 0.0 \pm 0.0	0.6 \pm 0.1 \pm 0.0 \pm 0.0	0.4 \pm 0.1 \pm 0.0 \pm 0.0	0.2 \pm 0.1 \pm 0.1 \pm 0.0										

Table 5: Nuclear modification factor $R_{p\text{Pb}}$ as a function of y with $p_{\text{T}} < 14 \text{ GeV}/c$. The first uncertainty is statistical, and the second one is the systematic component.

$R_{p\text{Pb}}$	$-4.0 < y < -2.5$	$2.5 < y < 4.0$
Prompt J/ψ	$0.93 \pm 0.03 \pm 0.07$	$0.62 \pm 0.01 \pm 0.04$
J/ψ from b	$0.92 \pm 0.05 \pm 0.12$	$0.78 \pm 0.02 \pm 0.09$
Inclusive J/ψ	$0.93 \pm 0.03 \pm 0.07$	$0.63 \pm 0.01 \pm 0.04$

Table 6: Forward-backward production ratio R_{FB} as a function of $|y|$ with $p_{\text{T}} < 14 \text{ GeV}/c$. The first uncertainty is statistical, and the second one is the systematic component.

R_{FB}	$2.5 < y < 3.0$	$3.0 < y < 3.5$	$3.5 < y < 4.0$
Prompt J/ψ	$0.72 \pm 0.05 \pm 0.07$	$0.62 \pm 0.03 \pm 0.04$	$0.64 \pm 0.04 \pm 0.04$
J/ψ from b	$0.92 \pm 0.11 \pm 0.09$	$0.84 \pm 0.08 \pm 0.08$	$0.72 \pm 0.09 \pm 0.07$
Inclusive J/ψ	$0.74 \pm 0.05 \pm 0.07$	$0.64 \pm 0.03 \pm 0.04$	$0.65 \pm 0.04 \pm 0.04$

Table 7: Forward-backward production ratio R_{FB} as a function of p_{T} with $2.5 < |y| < 4.0$. The first uncertainty is statistical, and the second one is the systematic component.

$p_{\text{T}} [\text{GeV}/c]$	R_{FB} (prompt J/ψ)	R_{FB} (J/ψ from b)	R_{FB} (inclusive J/ψ)
0.0 – 1.0	$0.62 \pm 0.06 \pm 0.04$	$0.84 \pm 0.18 \pm 0.07$	$0.63 \pm 0.06 \pm 0.04$
1.0 – 2.0	$0.58 \pm 0.04 \pm 0.04$	$0.97 \pm 0.15 \pm 0.16$	$0.61 \pm 0.04 \pm 0.04$
2.0 – 3.0	$0.60 \pm 0.04 \pm 0.04$	$0.85 \pm 0.12 \pm 0.15$	$0.62 \pm 0.04 \pm 0.04$
3.0 – 4.0	$0.66 \pm 0.04 \pm 0.04$	$0.96 \pm 0.14 \pm 0.12$	$0.69 \pm 0.04 \pm 0.04$
4.0 – 5.0	$0.75 \pm 0.06 \pm 0.05$	$0.89 \pm 0.16 \pm 0.14$	$0.76 \pm 0.05 \pm 0.05$
5.0 – 6.0	$0.75 \pm 0.07 \pm 0.05$	$0.77 \pm 0.16 \pm 0.06$	$0.75 \pm 0.07 \pm 0.05$
6.0 – 7.0	$0.77 \pm 0.08 \pm 0.05$	$0.91 \pm 0.22 \pm 0.15$	$0.78 \pm 0.09 \pm 0.05$
7.0 – 8.5	$0.83 \pm 0.11 \pm 0.06$	$1.08 \pm 0.27 \pm 0.11$	$0.87 \pm 0.11 \pm 0.06$
8.5 – 14	$0.67 \pm 0.10 \pm 0.05$	$0.74 \pm 0.19 \pm 0.06$	$0.68 \pm 0.09 \pm 0.04$

References

- [1] T. Matsui and H. Satz, *J/ψ suppression by quark-gluon plasma formation*, Phys. Lett. **B178** (1986) 416.
- [2] E. G. Ferreira, F. Fleuret, J. P. Lansberg, and A. Rakotozafindrabe, *Impact of the nuclear modification of the gluon densities on J/ψ production in pPb collisions at $\sqrt{s_{NN}} = 5$ TeV*, arXiv:1305.4569.
- [3] J. Albacete *et al.*, *Predictions for p+Pb collisions at $\sqrt{s_{NN}} = 5$ TeV*, Int. J. Mod. Phys. **E22** (2013) 1330007, arXiv:1301.3395.
- [4] F. Arleo and S. Peigne, *Heavy-quarkonium suppression in p-A collisions from parton energy loss in cold QCD matter*, JHEP **03** (2013) 122, arXiv:1212.0434.
- [5] F. Arleo, R. Kolevato, S. Peign, and M. Rustomova, *Centrality and p_{\perp} dependence of J/ψ suppression in proton-nucleus collisions from parton energy loss*, JHEP **05** (2013) 155, arXiv:1304.0901.
- [6] F. Arleo and S. Peigne, *J/ψ suppression in p-A collisions from parton energy loss in cold QCD matter*, Phys. Rev. Lett. **109** (2012) 122301, arXiv:1204.4609.
- [7] A. Adeluyi and T. Nguyen, *Coherent photoproduction of ψ and Υ mesons in ultraperipheral pPb and PbPb collisions at the CERN Large Hadron Collider at $\sqrt{s_{NN}} = 5$ TeV and $\sqrt{s_{NN}} = 2.76$ TeV*, Phys. Rev. **C87** (2013) 027901, arXiv:1302.4288.
- [8] G. A. Chirilli, B.-W. Xiao, and F. Yuan, *Inclusive hadron productions in pA collisions*, Phys. Rev. **D86** (2012) 054005, arXiv:1203.6139.
- [9] G. A. Chirilli, *High-energy QCD factorization from DIS to pA collisions*, Int. J. Mod. Phys. Conf. Ser. **20** (2012) 200, arXiv:1209.1614.
- [10] FNAL E866/NuSea collaboration, M. J. Leitch *et al.*, *Measurement of differences between J/ψ and ψ' suppression in p-A collisions*, Phys. Rev. Lett. **84** (2000) 3256, arXiv:nucl-ex/9909007.
- [11] HERA-B collaboration, I. Abt *et al.*, *Kinematic distributions and nuclear effects of J/ψ production in 920 GeV fixed-target proton-nucleus collisions*, Eur. Phys. J. **C60** (2009) 525, arXiv:0812.0734.
- [12] BRAHMS collaboration, I. Arsene *et al.*, *Evolution of the nuclear modification factors with rapidity and centrality in d + Au collisions at $\sqrt{s_{NN}} = 200$ GeV*, Phys. Rev. Lett. **93** (2004) 242303, arXiv:nucl-ex/0403005.
- [13] PHENIX collaboration, S. S. Adler *et al.*, *Nuclear modification factors for hadrons at forward and backward rapidities in deuteron-gold collisions at $\sqrt{s_{NN}} = 200$ GeV*, Phys. Rev. Lett. **94** (2005) 082302, arXiv:nucl-ex/0411054.

- [14] PHENIX collaboration, A. Adare *et al.*, *Cold nuclear matter effects on J/ψ yields as a function of rapidity and nuclear geometry in $d + A$ collisions at $\sqrt{s_{NN}} = 200$ GeV*, Phys. Rev. Lett. **107** (2011) 142301, [arXiv:1010.1246](#).
- [15] LHCb collaboration, A. A. Alves Jr. *et al.*, *The LHCb detector at the LHC*, JINST **3** (2008) S08005.
- [16] M. Adinolfi *et al.*, *Performance of the LHCb RICH detector at the LHC*, Eur. Phys. J. **C73** (2013) 2431, [arXiv:1211.6759](#).
- [17] A. A. Alves Jr. *et al.*, *Performance of the LHCb muon system*, JINST **8** (2013) P02022, [arXiv:1211.1346](#).
- [18] R. Aaij *et al.*, *The LHCb trigger and its performance in 2011*, JINST **8** (2013) P04022, [arXiv:1211.3055](#).
- [19] T. Sjöstrand, S. Mrenna, and P. Skands, *PYTHIA 6.4 physics and manual*, JHEP **05** (2006) 026, [arXiv:hep-ph/0603175](#).
- [20] I. Belyaev *et al.*, *Handling of the generation of primary events in GAUSS, the LHCb simulation framework*, Nuclear Science Symposium Conference Record (NSS/MIC) **IEEE** (2010) 1155.
- [21] D. J. Lange, *The EvtGen particle decay simulation package*, Nucl. Instrum. Meth. **A462** (2001) 152.
- [22] P. Golonka and Z. Was, *PHOTOS Monte Carlo: a precision tool for QED corrections in Z and W decays*, Eur. Phys. J. **C45** (2006) 97, [arXiv:hep-ph/0506026](#).
- [23] GEANT4 collaboration, J. Allison *et al.*, *Geant4 developments and applications*, IEEE Trans. Nucl. Sci. **53** (2006) 270; GEANT4 collaboration, S. Agostinelli *et al.*, *GEANT4: a simulation toolkit*, Nucl. Instrum. Meth. **A506** (2003) 250.
- [24] M. Clemencic *et al.*, *The LHCb simulation application, GAUSS: design, evolution and experience*, J. of Phys. : Conf. Ser. **331** (2011) 032023.
- [25] LHCb collaboration, R. Aaij *et al.*, *Measurement of J/ψ production in pp collisions at $\sqrt{s} = 7$ TeV*, Eur. Phys. J. **C71** (2011) 1645, [arXiv:1103.0423](#).
- [26] LHCb collaboration, R. Aaij *et al.*, *Measurement of J/ψ production in pp collisions at $\sqrt{s} = 2.76$ TeV*, JHEP **02** (2013) 41, [arXiv:1212.1045](#).
- [27] LHCb collaboration, R. Aaij *et al.*, *Production of J/ψ and Υ mesons at $\sqrt{s} = 8$ TeV*, JHEP **06** (2013) 64, [arXiv:1304.6977](#).
- [28] F. Archilli *et al.*, *Performance of the muon identification at LHCb*, [arXiv:1306.0249](#), submitted to JINST.

- [29] Particle Data Group, J. Beringer *et al.*, *Review of particle physics*, Phys. Rev. **D86** (2012) 010001, and 2013 partial update for the 2014 edition.
- [30] T. Skwarnicki, *A study of the radiative cascade transitions between the Upsilon-prime and Upsilon resonances*, PhD thesis, Institute of Nuclear Physics, Krakow, 1986, DESY-F31-86-02.
- [31] M. Pivk and F. R. Le Diberder, *sPlot: a statistical tool to unfold data distributions*, Nucl. Instrum. Meth. **A555** (2005) 356, [arXiv:physics/0402083](#).
- [32] A. Jaeger *et al.*, *Measurement of the track finding efficiency*, CERN-LHCb-PUB-2011-025.
- [33] LHCb collaboration, R. Aaij *et al.*, *Measurement of J/ψ polarization in pp collisions at $\sqrt{s} = 7$ TeV*, [arXiv:1307.6379](#), submitted to Eur. Phys. J. C.
- [34] S. van der Meer, *Calibration of the effective beam height in the ISR*, CERN report, CERN-ISR-PO-68-31 (1968).
- [35] H. Burkhardt and P. Grafström, *Absolute luminosity from machine parameters*, CERN report, CERN-LHC-PROJECT-REPORT-1019 (2007).
- [36] ALICE collaboration, B. Abelev *et al.*, *J/ψ production and nuclear effects in p -Pb collisions at $\sqrt{s_{NN}} = 5.02$ TeV*, CERN-PH-EP-2013-163, submitted to JHEP.